

Ultra Wide-Band Channel Characterization Using Generalized Gamma Distributions

Zakaria Mohammadi¹, Rachid Saadane^{1,2}, and Driss Aboutajdine¹

¹ GSCM-LRIT Laboratory Associated with CNRST,
Faculty of Science, University Mohammed V- Agdal, Rabat.

² LETI laboratory, Ecole Hassania des Travaux Publiques,
Km 7 Route d' El Jadida, B.P 8108, Casa-Oasis, Casablanca
Zakariamhm@gmail.com, rachid.saadane@ehpt.ac.ma,
aboutaj@fsr.ac.ma

Abstract. In this paper, we present an experimental characterization of the ultra-wide bandwidth (UWB) indoor channel using Generalized Gamma distributions. This investigation is also based on the analysis of the statistical properties of the multipath profiles when thresholding the estimated Power Delay Profile PDP over a spaced measurement grid. This characterization procedure was applied to the ultra wideband channel measurements collected from a measurement campaign, which has been performed within the whyless.com project by the IMST group, over a bandwidth of 10 GHz.

Keywords: Ultra Wideband, Power Delay Profile, Generalized Gamma distribution, Small Scale Fading, channel Modeling.

1 Introduction

The challenge of the recent communication systems is to field the user's requirement on low power consumption, little interferences with other systems, and high rate transmission. Therefore, ultra wideband (UWB) radio is an emerging technology, and has received great interest from the research and industry community, notably for Wireless Personal Area Network WPAN. It consists generally to transmit very short pulses, over a large frequency bandwidth, in the order of 500 MHz to several GHz, according to the specification of the Federal communication commission (FCC) [1]. However, an appropriate knowledge of the UWB channel proves necessary for the design, simulation, and performance evaluation of such systems. Many characterizations have been performed for several environments: Indoor, Outdoor, Corridor, Office... [2][3][4]. All this contributions are based on experimental measurements of the UWB channel. Many measurements campaigns have been performed within the past few years, mainly due to emerging UWB standards (e.g. multiband OFDM-UWB, IEEE 802.15.4a, and IEEE 802.15.3c). It can be done either in frequency or time domain. Usually, time domain sounding consists to the transmission of a pseudo-noise sequence and to estimate the channel impulse response by correlating the emitted sequence with the received one [5]. While this technique is

more suited to outdoor context, the frequency domain sounding is more adapted to indoor measurements, by using a Vector Network Analyzer VNA, which emits a series of tones with frequency f at Port 1 and measures the relative amplitude and phase with respect to Port 2, providing automatic phase synchronization between the two ports. This technique was performed by the IMST group using a frequency VNA to acquire indoor UWB channel data. The rest of this paper is organized as follow: The second section describes briefly The IMST measurements campaign setup, scenarios and estimation of the channel response. The Generalized Gamma (GG) distribution is presented in the third section, while we describe the procedure by which we processed the measured data to extract a set of model parameters, before evaluating and comparing the model with the available Power Delay Profile PDP.

2 Measurement Campaign

To study the characterization of the UWB channel using GG distribution, we worked with the IMST Data, collected from a measurement campaign done within the Whyless.com project, in frequency domain using a VNA in indoor environment as shown in Fig .1. We are also interested in only two scenarios: the Line Of Sight (LOS) and Non-Line Of Sight (NLOS). All the radio measurements have been performed at the IMST premise within an office with dimension $5\text{m} \times 5\text{m} \times 2.6\text{m}$. The office has a single door, one wall with windows, and contains a metal cabinet. Both the transmitter and receiver deploy a bi-conical horn antenna with approx. 1dBi gain, positioned at a height of 1.5m. The attenuation and the phase of the channel response have been measured from 1 to 11 GHz with 6.25 MHz frequency spacing. The measurement process is described more in detail in [6]. We denote by local PDP the Power Delay profile measured at a fixed Receiver Rx and transmitter Tx distance, given as $PDP(\tau, d) = |h(\tau, d)|^2$. The small scale effects are then shown in the variation of the measured PDP caused by small change of the transmitter position.

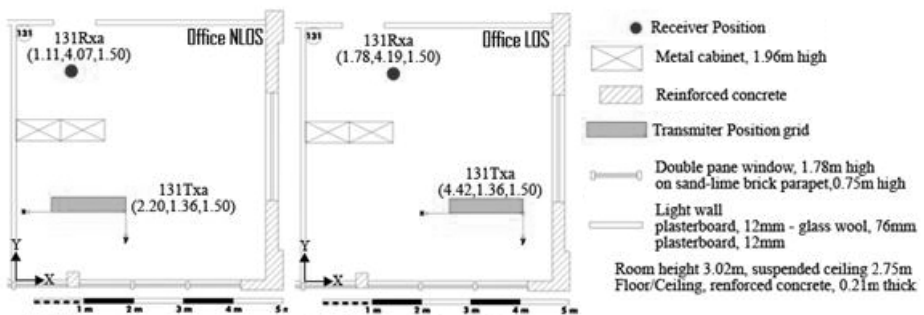


Fig. 1. Measurements Campaign Scenarios

Globally, the Tx position changes over a rectangular grid $150\text{cm} \times 30\text{cm}$ with a spatial resolution $\Delta d = 1\text{cm}$, resulting with a total of 4530 PDPs. Since the PDP amplitude vary when changing the Tx-Rx distance d , we proceed to a normalization of the PDPs with

respect to the first Multipath Component MPC arrival time, determined as $\tau_{\text{ref}} = d/c$, where c is the speed of light. Then it was identified as the origin of the delay axis. The goal of this normalization is to use the averaging technique safely, by anticipating the effect of smearing for an accurate extraction of statistical parameters.

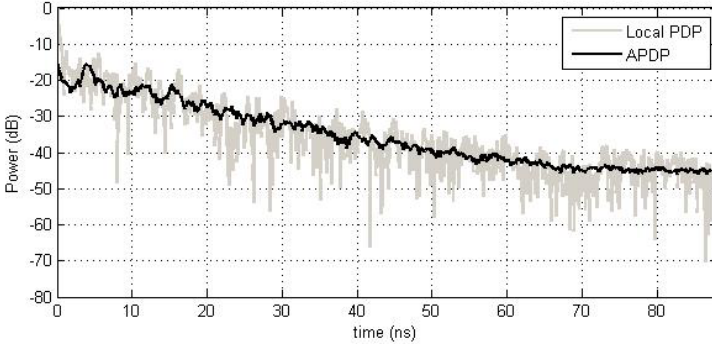


Fig. 2. Example of normalized estimated LOS-APDP in logarithmic scale

3 Generalized Gamma Distribution

Because of its flexibility and high quality adjustment, the Generalized Gamma Distribution was used in many fields like signal & image processing, mobile communication and many others. It was first introduced in [7]. The GGD Probability Density Function PDF is defined as follows:

$$f(x; \alpha, \beta, k, \gamma) = \frac{k(x-\gamma)^{k\alpha-1} \exp\left(-\left(\frac{x-\gamma}{\beta}\right)^k\right)}{\beta^{k\alpha} \Gamma(\alpha)} \quad (1)$$

For $\gamma \leq x < +\infty$, where α and k are the positive real valued shape parameters, β the continuous scale parameter ($\beta > 0$), γ the location parameter ($\gamma = 0$ yields the three parameters GGD) and $\Gamma(\bullet)$ is the Gamma function. Among the interesting properties of this distribution, it has one more parameter than the most used distributions rendering it more flexible to the measurement data, moreover it contains a large variety of other distributions for different values of scale and shape parameters: Rayleigh ($k=2, \alpha=1$), exponential ($k=1, \alpha=1$), Nakagami ($k=2$), Gamma ($k=1$), log-normal ($\alpha \rightarrow \infty$), and Weibull ($\alpha=1$). For assessing the goodness of fit, we have to estimate the model-parameters. Since the APDPs values are all positive, the location parameter γ is assumed zero-valued ($\gamma=0$). To estimate the parameters α, β and k , we adopt the Maximum Likelihood ML method. Assuming $X = \{X_1, X_2, \dots, X_N\}$ a vector of mutually independent data, the Log likelihood is expressed as:

$$\begin{aligned} L(X; \alpha, \beta, k) &= \log f_x(X; \alpha, \beta, k) \\ &= N \log \left(\frac{k}{\beta^{k\alpha} \Gamma(\alpha)} \right) + (\alpha k - 1) \sum_{i=1}^N \log(x_i) - \sum_{i=1}^N \left(\frac{x_i}{\beta} \right)^k. \end{aligned} \quad (2)$$

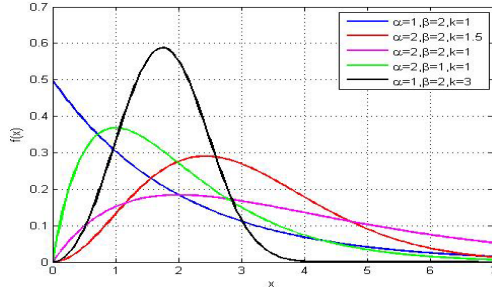


Fig. 3. PDF of the GID with $\gamma=0$ for different values of α , β and k

By settings the derivative of this function with respect to α , β and k to zero, we obtain the expression of the Maximum Likelihood ML estimators for the three parameters. Specifically, the expression of the estimators is:

$$\frac{\partial L(X; \alpha, \beta, k)}{\partial \alpha} = -N(k \log(\beta) - \psi(\alpha)) + \sum_{i=1}^N k \log(x_i) = 0, \psi(z) = \frac{\Gamma'(z)}{\Gamma(z)}. \quad (3)$$

$$\frac{\partial L(X; \alpha, \beta, k)}{\partial k} = N \left(\frac{1}{k} - \alpha \log(\beta) \right) + \sum_{i=1}^N \alpha \log(x_i) - \left(\frac{x_i}{\beta} \right)^k \log \frac{x_i}{\beta} = 0. \quad (4)$$

$$\frac{\partial L(X; \alpha, \beta, k)}{\partial \beta} = -\frac{N\alpha k}{\beta} + \frac{k\beta^{-k}}{\beta} \sum_{i=1}^N x_i = 0. \quad (5)$$

Then the estimators can be straightforwardly determined by solving a three equations system [8]. After computing the estimated parameters, we use the test of Kolmogorov Smirnov [9] to evaluate the Goodness-Of-Fit of the fitted distribution regarding the data-set. It consists to test how well a hypothesized distribution function $F(x)$ fits an empirical distribution function $F_n(x)$, which equals the fraction of x_i that are less than or equal to x for each $-\infty < x < +\infty, i.e.$

$$F_n(x) = \frac{1}{n} \sum_{i=1}^n I_{\{x_i \leq x\}} \quad (6)$$

One of the simplest measures is the largest distance between the two functions $S(x)$ and $F(x)$, measured in a vertical direction. This statistic was suggested by Kolmogorov, and was used in our simulations for evaluating quality of adjustment.

4 Simulations and Results

In the majority of results, the power of APDP varies in logarithmic scale between 0db and -50db with respect to the strongest MPC arrived at τ_{ref} . The first simulation consists to apply several thresholds to the APDPs and computing the number of

MPCs arriving within the cut-off threshold. The usual thresholding processing comprises cutting off all data below a previously determined threshold and keep only the MPCs above it. In this simulation, the average MPCs number was calculated for several threshold values in both scenarios. We can observe an increase of the MPCs number when decreasing the threshold value. Then it is possible to estimate the total energy carried by the thresholded APDP. The large values of captured energy indicate that the temporal dispersion parameters can be estimated accurately, as denoted in [10]. Otherwise, this will enhance the estimation of temporal parameters when the total energy captured is more than 90%. Then the APDPs can be cutting-off using appropriate thresholds. The adopted threshold was -45dB and -35dB for LOS and NLOS respectively, corresponding to average MPCs number of 720 and 780 components. Then the 45 resulting APDPs are referred to our GFD-Model using the ML estimator to extract different values of shape and scale parameters. It was found that the Log-Logistic distribution gives the best agreement with the empirical distribution of the shape parameter α for different APDPs delay bin in both scenarios. Previous results showed that the 45 shape parameters α values are well modeled as log-logistic, denoted as $\text{LL}(\alpha, \beta, \gamma)$ with $(\alpha=92.869, \beta=0.68477, \gamma=0.32788)$ for LOS, while $(\alpha=39.336, \beta=0.24988, \gamma=0.75758)$ for NLOS. The table 1 shows the goodness of fit using the test of Kolmogorov-Smirnov for Log-Logistic, Normal, Log-Normal and Nakagami, which gives the best values of KS test. The histograms of the experimental α and the theoretically fitted distribution are shown in Fig.4. Applying the same procedure to characterize the second shape parameter k , we found that it is also log-normally and log-logistically distributed for LOS and NLOS respectively, i.e. $k_{\text{LOS}} \approx \text{LN}(\sigma=1.6589, \mu=-6.8785, \gamma=8,0738 \text{ E-}5)$, and $k_{\text{NLOS}} \approx \text{LL}(\alpha=1,0781, \beta=0,00339, \gamma=4,9560 \text{ E-}4)$, while assuming that the large values of parameter k correspond to the first multipath components, and the small k -values are associated with the later MPCs, with respect to linear fitting value for both scenarios.

Table 1. Goodness-Of-Fit for shape parameter α

		Log-Logistic (α, β, γ)	Normal (σ, μ)	Log-Normal (σ, μ, γ)	Nakagami (m, Ω)
LOS	Statistic	0.0541	0.09914	0.09785	0.09923
	Distribution Parameters	(92.869, 0.68477, 0.32788)	(0.01531, 1.0131)	(0.01512, 0.01293, 0.32168)	(1096.6, 1.0267)
NLOS	Statistic	0.02979	0.04217	0.0388	0.04159
	Distribution Parameters	(39.336, 0.24988, 0.75758)	(0.01164, 1.0079)	(0.02807, -0.8761, 0.5913)	(1874.1, 1.0159)

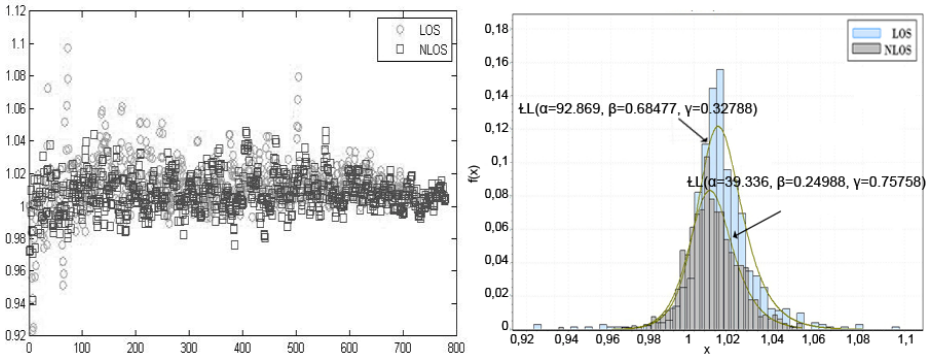


Fig. 4. Values and histograms of the shape parameter α and the theoretically fitted distribution

The previous shape parameters determine the shape of the distribution, while the scale parameter β determine the statistical dispersion of the probability distribution. If β presents large values, the distribution will be more spread out. Otherwise, the distribution will be more concentrated. The results indicate that the first LOS delay bins are more expanded than the others, whereas we notice that as far as the bin index increases, for LOS and NLOS scenarios, the bin values becomes more spread. This can be seen through FIG.5. Note that using the K-S test, we find that the scale parameter follows a Log-Logistic distribution for LOS scenario $\beta_{LOS} \approx \text{LL}(\alpha=2.829, \beta=15.91, \gamma=0.95684)$, while it is Log-Normally distributed for NLOS $\beta_{NLOS} \approx \text{LN}(\sigma=0.24244, \mu=3.2558, \gamma=-7.7394)$.

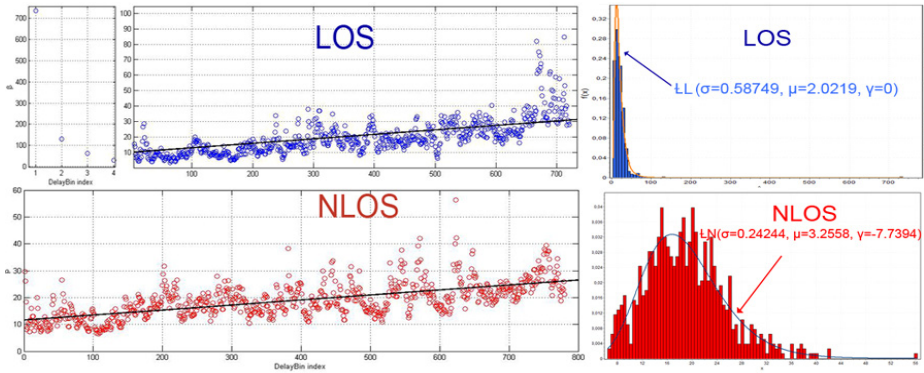


Fig. 5. Values and histograms of β with the theoretically fitted distributions

Then, it is possible to build simulated channel responses according to our simulation procedure, as described in FIG.6. In the model described above, the different shape and scale parameters are modeled with Log-Logistic or Log-Normal distributions, depending on the scenarios to simulate. The FIG.7 shows an example of comparison between a resulted APDP from our model with experimental one. It can be shown that the resulted Averaged Power Delay Profile reproduce roughly the same trend of our experimental data.

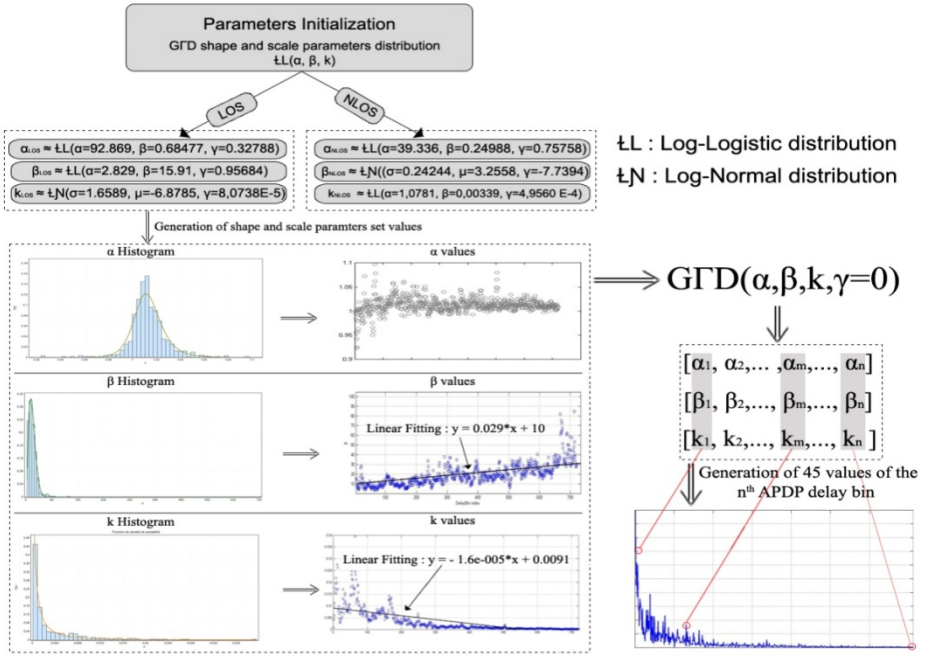


Fig. 6. Flowchart of the procedure for generating simulated APDP

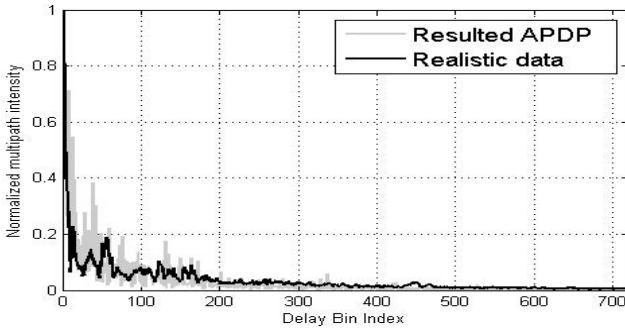


Fig. 7. Example of simulated VS Realistic APDP in LOS scenario

For the moment, the qualitative visual inspection remains the used method to evaluate the quality of modeling, while there are several other ways to assess the proposed model. Among them, quality of signal, calculated by integrating the theoretical and the modeled APDPs over all delays bin. This technique remains sometimes inaccurate, because of possibility of signal amplification which can affect its quality. However, the most used technique consists to compare some temporal parameters between the experimental response and the result built with the proposed model. More precisely, most authors use the Root mean square (RMS) delay spread

τ_{RMS} as a significant value which provide the time dispersion and the frequency selectively of the Power Delay Profile due to Multipath propagation. Moreover, to improve our model, we can enhance our flowchart by introducing some modification of our modeling process: for example, the linear fitting for the shape and scale parameters k and β proves be less suitable to describe the ascending and descending trend of this parameters. For this reason, we can use exponential or polynomial fitting.

5 Conclusion

In this paper, we performed a statistical analysis of UWB channel realizations, obtained from a measurement campaign in an indoor office environment using the parametric Generalized Gamma Distribution. Based on these results, we proposed a statistical model for generating UWB propagation channel. The experiment shows that the resulted channel Power Delay Profile can reproduce the same trend of the real channel response. In this work, we are limited to evaluate the quality of modeling with visual inspection, while we expected to improve our basic model and to assess our model using more developed tools are discussed before in future works.

References

1. Federal Communication Commission (FCC): First Report and Order in the Matter of Revision of Part 15 of the Commission's rule regarding Ultra-wideband transmission Systems. ET-Docket 98-153, FCC 02-48 (released, April 2002)
2. Uday, N., Kantz, K., Viswanathany, R., Cheung, D.: Characterization of Ultra Wideband Communications in Data Center Environments. In: IEEE International Conference on Ultra-wideband, Singapore (September 2007)
3. Alvarez, A., Valera, G., Lobeira, M., Toress, R., Garcia, J.L.: Ultra wideband channel characterization and modeling. In: Proc. Int. Workshop on Ultra Wideband Systems, Oulu, Finland (June 2003)
4. Rusch, L., Prettie, C., Cheung, D., Li, Q., Ho, M.: Characterization of UWB propagation from 2 to 8 GHz in a residential environment. IEEE Journal on Selected Areas in Communications (submitted for publication)
5. Rappaport, T.S.: Wireless Communications - Principles and Practice. Prentice Hall PTR, Upper Saddle River
6. Kunisch, J., Pamp, J.: Measurement results and modeling aspects for UWB radio channel. In: Proc. of IEEE Conference Ultra Wideband Systems and Technologies, pp. 19–23 (2002)
7. Stacy, E.W.: A generalization of the Gamma distribution. Ann. Math. Statist. 33(3), 1187–1192 (1962)
8. Chang, J.H., Shin, J.W., Kim, N.S., Mitra, S.K.: Image Probability Distribution Based on Generalized Gamma Function. IEEE Signal Process. Lett. 12(4), 325–328 (2005)
9. D'Agostino, R., Stephens, M.: Goodness-of-Fit Techniques (Marcel Dekker) (1986)
10. Molisch, A.F., Cassioli, D., Chong, C.C., Emami, S., Fort, A., Kannan, B., Karedal, J., Kunisch, J., Schantz, H.G., Siwiak, K., Win, M.Z.: A comprehensive standardized model for UWB propagation channels. IEEE Trans. Antennas and Propagation 54(11), 3151–3166 (2006)